

1 Nucleus specific expression in the multinucleated mushroom-
2 forming fungus *Agaricus bisporus* reveals different nuclear
3 regulatory programs

4 Thies Gehrman^{1,*}, Jordi F. Pelkmans², Robin A. Ohm², Aurin M. Vos^{2,#}, Anton S.M.
5 Sonnenberg³, Johan J.P. Baars³, Han A. B. Wösten², Marcel J. T. Reinders¹, Thomas Abeel^{1,4,\$}

6 ¹Delft Bioinformatics Lab, Delft University of Technology, The Netherlands

7 ²Fungal Microbiology, Utrecht University, The Netherlands

8 ³Plant Breeding, Wageningen University and Research, The Netherlands

9 ⁴Broad Institute of MIT and Harvard, USA

10 *Current position: CBS/KNAW Westerdijk Fungal Biodiversity Institute, The Netherlands

11 #Current position: Department of Biotechnology, Delft University of Technology, The
12 Netherlands

13 \$Corresponding author: T.Abeel@tudelft.nl

14

15 **Abstract**

16 **Motivation:** Fungi are essential in nutrient recycling in nature. They also form symbiotic,
17 commensal, parasitic and pathogenic interactions with other organisms including plants, animals
18 and humans. Many fungi are polykaryotic, containing multiple nuclei per cell. In the case of
19 heterokaryons, there are even different nuclear types within a cell. It is unknown what the
20 different nuclear types contribute in terms of mRNA expression levels in fungal heterokaryons.
21 Each cell of the cultivated, mushroom forming basidiomycete *Agaricus bisporus* contains 2 to 25
22 nuclei of two nuclear types that originate from two parental strains. Using RNA-Seq data, we
23 wish to assess the differential mRNA contribution of individual nuclear types in heterokaryotic
24 cells and its functional impact.

25 **Results:** We studied differential expression between genes of the two nuclear types throughout
26 mushroom development of *A. bisporus* in various tissue types. The two nuclear types, *P1* and *P2*,
27 produced specific mRNA profiles which changed through development of the mushroom. The
28 differential regulation occurred at the gene level, rather than at locus, chromosomal or nuclear
29 level. Although the *P1* nuclear type dominates the mRNA production throughout development,
30 the *P2* type showed more differentially upregulated genes in important functional groups
31 including genes involved in metabolism and genes encoding secreted proteins. Out of 5,090
32 karyolelle pairs, i.e. genes with different alleles in the two nuclear types, 411 were differentially
33 expressed, of which 246 were up-regulated by the *P2* type. In the vegetative mycelium, the *P2*
34 nucleus up-regulated almost three-fold more metabolic genes and cazymes than *P1*, suggesting
35 phenotypic differences in growth. A total of 10% of the differential karyollele expression is
36 associated with differential methylation states, indicating that epigenetic mechanisms may be
37 partly responsible for nuclear specific expression.

38 **Conclusion:** We have identified widespread transcriptomic variation between the two nuclear
39 types of *A. bisporus*. Our novel method enables studying karyolletle specific expression which
40 likely influences the phenotype of a fungus in a polykaryotic stage. This is thus relevant for the
41 performance of these fungi as a crop and for improving this species for breeding. Our findings
42 could have a wider impact to better understand fungi as pathogens. This work provides the first
43 insight into the transcriptomic variation introduced by genomic nuclear separation.

44 **Introduction**

45 Fungi are vital to many ecosystems, contributing to soil health, plant growth, and nutrient
46 recycling¹. They are key players in the degradation of plant waste^{2,3}, form mutually beneficial
47 relationships with plants by sharing minerals in exchange for carbon sources^{4,5} and by inhibiting
48 the growth of root pathogens^{6,7}. They even form networks between plants, which can signal each
49 other when attacked by parasites⁸. Yet, some are plant pathogens responsible for huge economic
50 losses in crops⁹⁻¹¹.

51 The genome organization of fungi is incredibly diverse and can change during the life cycle. For
52 instance, sexual spores can be haploid with one or more nuclei or can be diploid. Sexual spores
53 of mushroom forming fungi are mostly haploid and they form monokaryotic (one haploid
54 nucleus per cell) or homokaryotic (two or more copies of genetically identical haploid nuclei)
55 mycelia upon germination. Mating between two such mycelia results in a fertile dikaryon (one
56 copy of the parental nuclei per cell) or heterokaryon (two or more copies of each parental nuclei)
57 when they have different mating loci¹². In contrast to eukaryotes of other kingdoms, the nuclei
58 do not fuse into di- or polyploid nuclei but remain side by side during the main part of the life

59 cycle. Only just before spores are formed in mushrooms, do these nuclei fuse, starting the cycle
60 anew.

61 *Agaricus bisporus* is the most widely produced and consumed edible mushroom in the world².
62 Heterokaryotic mycelia of the button mushroom *Agaricus bisporus* var. *bisporus* (Sylvan A15
63 strains) have between 2 and 25 nuclei per cell^{13,14} (Figure 1). The genomes of both ancestral
64 homokaryons have been sequenced^{1,15} showing that DNA sequence variation is associated with
65 different vegetative growth capabilities¹. Due to the two nuclear types, each gene exists at two
66 alleles separated by nuclear membranes, which we call karyolleles. Although there have been a
67 few studies investigating the expression of genetic variety in the transcriptome^{16,17}, the
68 differential transcriptomic activity of two (or more) nuclear types has never been systematically
69 investigated in a heterokaryon at the genome wide scale. Based on SNPs identified in mRNA
70 sequencing, it has been suggested that allele specific expression is tightly linked to the ratio of
71 the nuclear types in a basidiomycete¹⁸.

72 Allele specific expression in mononuclear cells has been studied in fungi¹⁹, plants²⁰, animals²¹,
73 and humans²². Such studies have shown that allele heterogeneity is linked to differential allele
74 expression and cis-regulatory effects²¹⁻²³, and even sub-genome dominance²⁴. *A. bisporus* is in
75 many ways an excellent model organism to investigate differential karyollele expression. It only
76 has two nuclear types in the heterokaryon contrasting to the mycorrhizae that can have more
77 nuclear types^{25,26}, making computational deconvolution of mRNA sequence data intractable with
78 currently available tools. Additionally, the recently published genomes of the two nuclear types
79 of *Sylvan A15*¹⁵ exhibit a SNP density of 1 in 98 bp allowing differentiation of transcripts in high
80 throughput sequencing data. Finally, bulk RNA-Seq datasets of different stages of development
81 and of different tissues of the fruiting bodies are available^{2,27}.

82 Here, we show that differential karyollele expression exists in *Agaricus bisporus* *Sylvan A15*
83 strain, which changes across tissue type and development and affects different functional groups.
84 Further, we show that differential karyollele expression associates with differential methylation
85 states, suggesting that epigenetic factors may be a cause for the differential regulation of
86 karyolleles.

87 **Results**

88 **Karyollele specific expression through sequence differences**

89 To assign expression levels to individual karyolleles, we exploit sequence differences between
90 karyollele pairs in the P1 and P2 homokaryon genomes of *A. bisporus* *A15* strain (Materials).
91 Briefly, the sequence differences define marker sequences for which the RNA-Seq reads
92 uniquely match to either the P1 or the P2 variant, effectively deconvolving the mRNA
93 expression from the two nuclear types (see Methods). There are a total of 5,090 distinguishable
94 karyollele pairs between the *P1* and *P2* genomes, corresponding to ~46% of all genes. The
95 remaining genes could not be unambiguously matched, or the karyollele pairs had too few
96 sequences differences. Most (80%) distinguishable karyollele pairs had the same number of
97 markers in each homokaryon. For the remaining pairs (20%), the number of markers per
98 karyollele was different (see Supplementary Material Note A). This variation can be explained
99 by the non-symmetric number of markers produced by the different kinds of variation. While a
100 SNP will result in one marker in each karyollele, an indel (if longer than 21bp) will result in one
101 marker in one karyollele, and at least two in the other. Karyollele specific expression is
102 expressed as a read count ratio that reflects the relative abundance of mRNAs originating from
103 the P1 or P2 nuclear types (Equation 3, Methods).

104 We studied *A. bisporus*' karyollele specific expression for different tissues and development in
105 two RNA-Seq datasets, one studying the mycelium in compost throughout mushroom harvest,
106 and one studying different mushroom tissues throughout mushroom formation (Figure 2,
107 Supplementary Material Note C, and Materials). Measured difference in expression between
108 nuclear types is not correlated with the number of markers ($p > 0.05$) for any of the samples, nor
109 is it correlated with CG content (see Supplementary Material Note B).

110 **P1 and P2 mRNA production differs per tissue and across development**

111 First, we assess the total mRNA production of the P1 and P2 nuclear types and their relative
112 contributions during development. To do this, we considered the total number of reads uniquely
113 matching to P1 with respect to P2. Figure 2 shows that this nuclear type read count ratio (NRR,
114 see Equation 5, Methods) changes throughout development and across tissue types. For example,
115 during the '*Differentiated*' stage, the P2 nuclei are dominant in the skin, but in the '*Young*
116 '*Fruiting Body*', the P1 nuclei dominate the skin (two right most panels in Figure 2). In contrast,
117 the '*Stipe Center*' is dominated by P1 nuclei in the differentiated stage, while later the expression
118 of P2 nuclei dominates.

119 The transcription patterns throughout the mushroom development differ between the karyolleles.
120 Based on a principal component analysis of the expression profiles of each nuclear type, we
121 observe that the expression profiles of P1 and P2 group together in different clusters, based on
122 the first and second principal components (Supplementary Material Note D). This clustering is
123 indicative of distinct regulatory programs. It appears as though the first principal component
124 represents the tissue type, and the second represents the nuclear type. Interestingly,
125 measurements of the same tissue from P1 and P2 do not have exactly the same value for the first

126 principal component, indicating that the difference in nuclear type does not entirely explain the
127 variation between P1 and P2.

128 **Within a sample, mRNA production of P1 and P2 vary between chromosomes**

129 Figure 3 shows the Chromosome Read count Ratios (CRR, Equation 4), demonstrating that some
130 chromosomes are more active in P1 (e.g. chromosome 8) throughout development, while others
131 are more active in P2 (e.g. chromosome 9). Expression of other chromosomes depend on the
132 developmental state, changing in time (e.g. chromosome 2). The chromosome log₂ fold changes
133 lie between [-0.60, 0.79]. In the vegetative mycelium we see less drastic differences in mRNA
134 production throughout development than in the mushroom tissues, with expression log₂ fold
135 changes between [-0.28, 0.36] (see Supplementary Material Note C).

136 **A few highly expressed genes represent a large component of chromosome mRNA activity**

137 In Figure 3, we showed that more mRNA originates from P2 in the case of, for example,
138 chromosome 9 than from P1. This was in part due to a few genes which were very highly
139 expressed. These highly expressed genes skew the read count ratios (see Supplementary Material
140 Note E). The differences can be quite extreme; In one case, a P1 karyollele accounted for <1% of
141 all reads originating from chromosome 9, while its P2 karyollele accounted for 21% of all the
142 chromosome 9 reads. Hence, most of the observed differences for chromosome 9 (Figure 3) is
143 explained by such highly expressed genes (Supplementay Note F).

144 In total, we identified 22 genes whose contribution exceeds 10% of the total expression of the
145 chromosome it is located on. Most of these genes are differentially expressed between the two
146 nuclear types, with 16 showing fold changes larger than 2 (Supplementary Material Note F).

147 These genes are primarily metabolic.

148 **Gene read ratios reveal a dominant P1 type in mushroom tissue, but not in mycelium**

149 To investigate whether either nuclear type is truly dominant we correct for extremely highly
150 expressed genes by limiting their impact on the chromosome and tissue level ratios by using per-
151 gene activity ratios per chromosome (CGR, Equation 6), instead of read ratios. This revealed
152 that, in addition to P1 producing more mRNA than P2, P1 karyolleles were also more frequently
153 higher expressed than their P2 counterpart (Figure 4). Looking across all tissues and
154 chromosomes, P1 is significantly dominant over P2, i.e. the average of the log-transformed CGR
155 is significantly larger in the P1 nuclear type than the P2 nuclear type, following a t-test in
156 mushroom tissue, with $p < 0.01$, (see Supplementary Material Note G). Using the Chromosome
157 Gene Ratio has a notable impact on chromosome 9. Although P2 produces most chromosome 9
158 mRNA (Figure 3), it is not the case that more P2 karyolleles are more highly expressed than P1
159 karyolleles.

160 We do not observe such a dominance of P1 in the mycelium ($p > 0.05$, with t-test as in
161 mushroom dataset), where neither P1 nor P2 show a dominant mRNA activity (see
162 Supplementary Material Note H).

163 **A substantial portion of karyolleles are differentially expressed**

164 In each tissue, we determined the set of karyolleles which are statistically significantly
165 differentially expressed between the two nuclear types. Although the dominance of the P1
166 nuclear type indicates a general trend of higher activity across many genes, some karyollele pairs
167 have a much larger difference pointing towards a functional role. In total, we find 411 genes that
168 are differentially expressed (see Methods) in a mushroom tissue or in vegetative mycelium
169 throughout development (Table 1); 368 genes are differentially expressed in mushroom tissues,

170 and 82 in the vegetative mycelium. Interestingly, when a karyollele pair is differentially
171 expressed, with only a few exceptions (see Supplementary Material Note I), it will always be
172 observed to be more highly expressed in the same nuclear type, i.e. if a gene is observed to be
173 more highly expressed in P1 than in P2, than it will never be observed to be more highly
174 expressed in P2 than in P1 in other tissues, and vice versa. The only exceptions to this rule lie in
175 the set of genes that are differentially expressed in both the mushroom dataset and the mycelium
176 dataset.

177 The set of differentially higher expressed genes between the nuclear types in mushroom and
178 mycelium sets overlap with only 39 genes. In this intersection set, more genes are higher
179 expressed in P2 than in P1. Ten genes had a higher expression in P1, and 24 had a higher
180 expression in P2. Five were more highly expressed in P2 in the mycelium, but switched their
181 origin of primary expression to P1 in the mushroom (see Supplementary Material Note I). The
182 lack of a substantial overlap of differentially expressed genes between the two nuclear types is
183 indicative of different regulatory processes during the vegetative stage and a mushroom stage.

184 Although P2 upregulates more differentially expressed genes than P1 does, more genes show a
185 consistently higher expression in P1 than in P2. We identify consistently higher expressed genes
186 that show a higher expression in one nuclear type over the other across all samples (Methods). In
187 the mushroom tissue dataset, we find 1,115 genes that are consistently higher expressed in P1,
188 and 785 genes that are consistently higher expressed in P2. Similarly, in the vegetative
189 mycelium, we find 832 genes that are consistently higher expressed in P1 and 645 that are
190 consistently higher expressed in P2. The two datasets overlap with 470 and 256 genes for P1 and
191 P2, respectively.

192 **Table 1: Karyolleles differentially expressed between P1 and P2 in mushroom tissue and vegetative mycelium across**
193 **development. In the first row we indicate the number of differentially expressed genes that are higher expressed in the**
194 **different nuclear types for the two datasets (columns). The second row gives the total number of differentially expressed**
195 **genes in the two different datasets. Row three shows the number of differentially expressed genes in a dataset that are not**
196 **differentially expressed in the other dataset. In the last row, we show the number of differentially expressed genes that**
197 **overlap between the two datasets.**

	Mushroom tissue dataset		Mycelium tissue dataset	
	P1 up	P2 up	P1 up	P2 up
Diff. ex.	176	193	30	52
Total/dataset	368		82	
Unique/dataset	329		43	
Overlap	39 (411 total)			

198

199 **Co-localized gene clusters are co-regulated**

200 To investigate the level at which genes are regulated, we investigated whether there are regions
201 where the majority of genes were consistently higher expressed in one homokaryon than in the
202 other. We detected many of such regions, given in Table 2 and Figure 5 (Methods,
203 Supplementary Material Note J), hinting towards a sub-chromosomal level of regulation. This is
204 supported by observations in Figures 3 and 4, where we see that within one tissue chromosomes
205 are differently regulated, excluding a regulation at the nuclear level. Because we observe that co-
206 regulated gene are co-localized in regions, regulation can also not occur at the chromosome
207 level, because then we would have expected regions of co-regulation of the size of whole
208 chromosomes.

209 Co-regulated regions are more frequently upregulated for the P1 karyollele than for the P2
210 karyolleles. This observation is in agreement with the observed P1 nuclear type dominance. We
211 observe relatively little overlap between the Mushroom and Vegetative Mycelium datasets

212 (Table 2), indicative of different regulatory programs between the vegetative mycelium and
213 mushroom tissue cells.

214 **Table 2: The number of regions in which the majority of the genes are coregulated (Methods), across the mushroom and**
215 **mycelium datasets and with the number of genes in these regions. P1 and P2 columns indicate whether the region is**
216 **consistently higher in for the P1 karyollele or the P2 karyollele, respectively. Row *Both* indicates overlapping regions**
217 **between the mushroom and vegetative mycelium datasets. Supplementary Material Note J offers detailed expression**
218 **profiles of these regions.**

Dataset	P1		P2	
	#Regions	#Genes	#Regions	#Genes
Mushroom	207	741	73	233
Vegetative Mycelium	414	1955	43	140
Both	151	484	7	17

219

220 **Manganese Peroxidase is up-regulated in vegetative mycelium by P2, but in mushroom by**
221 **P1**

222 Of 90 genes with named annotations in *A. bisporus* (see Methods), 42 are identified as
223 differentiable karyollele pairs, and one, manganese peroxidase (*mnp1*) was differentially
224 expressed between the two nuclear types in any stage of development. *mnp1* is known to be
225 highly expressed in early stages of development, and drops to much lower levels (log fold
226 change of -2.8) after mushroom formation^{2,28}. In our datasets, the individual contributions of P1
227 and P2 to *mnp1* expression are largely different. In the vegetative mycelium, we find that P2
228 produces four-fold more *mnp1* immediately before mushroom formation than P1 (see
229 Supplementary Material Note K). In the mushroom tissue, however, *mnp1* is expressed on
230 average 4.2-fold higher by P1 in the stem of the fruiting body throughout development (see
231 Supplementary Material Note K). Whether this switching behavior is functionally relevant

232 remains unclear, as two karyolleles of *mnp1* have the same protein domain annotations in the P1
233 and P2 homokaryon genomes.

234 **Broad range of functionality affected by karyollele specific expression throughout**
235 **development**

236 Next, we set out to examine the functional annotations of the differentially expressed karyollele
237 pairs, considering the following categories: (i) transcription factors, (ii) metabolic genes, (iii)
238 secondary metabolism genes, (iv) cytochrome P450 genes, (v) carbohydrate active enzymes
239 (cazymes) and (vi) secreted proteins. These categories, with the exception of secondary
240 metabolite genes, are all enriched in the set of differentiable genes ($p < 0.05$ by a chi-squared
241 approximation to the fisher's exact test with FDR correction).

242 Figures 6 and 7 show the division of the 411 differentially expressed genes across the functional
243 categories in all the different samples. None of the differentially expressed genes were
244 transcription factors. For the other functional categories, we saw a more or less equal amount of
245 up-regulated karyolleles in P1 and P2 (Figure 6) in the mushroom tissues (except the vegetative
246 stage), and a more skewed distribution of activity in the mycelium dataset (and the vegetative
247 stage of the mushroom dataset). In these cases, P2 had more differentially expressed genes in
248 these functional categories (Figure 7).

249 The P2 type had a higher expression of significantly more karyolleles than P1 in mycelium (see
250 Supplementary Material Note L). In the mycelium, P2 had an enriched expression of cytochrome
251 P450 genes, secondary metabolite genes, and cazymes ($p < 0.05$, with an FDR corrected chi-
252 squared approximation to the fisher's exact test). Furthermore, cazymes and metabolic genes in

253 mycelium were more likely to be more highly expressed in P2 ($p < 0.05$, with an FDR corrected
254 binomial test).

255 Nineteen of the 39 previously identified differentially expressed genes that are shared between
256 the mycelium and mushroom datasets had the following functional annotations: 14 were
257 annotated as metabolic genes, 14 as cazymes, five as secreted proteins, and two as cytochrome
258 P450s (some genes have multiple annotations). Additionally, five of these 39 overlapping genes
259 have different domain annotations, indicating different functional properties between the P1 and
260 P2 karyolleles.

261 To further elucidate the functional impact of the 411 differentially expressed genes, we mapped
262 them onto the KEGG pathway database. Sixteen of the genes that are differentially expressed in
263 mushroom tissue or vegetative mycelium samples are found in 20 pathways. Interestingly, three
264 differentially expressed genes are found in the Aminoacyl-tRNA biosynthesis (M00359)
265 pathway (Supplementary Material Note M). Two genes belong to valine and methionine tRNAs
266 pathways and were upregulated in P1. One gene in the pathway producing aspartamine tRNAs
267 pathway was upregulated in P2. Together, this suggests that P1 is able to produce more valine
268 and methionine tRNAs than P2.

269 Next we studied whether differential expression of a karyollele also resulted in the production of
270 a functionally different protein due to sequence differences between the karyolleles. 216 of the
271 5,090 distinguishable karyolleles had sequence differences that led to an alternative protein
272 domain annotation, and 36 of these 216 have alternative domain annotations. 36 of these 216
273 karyollele pairs are differentially expressed between P1 and P2 (see Supplementary Material
274 Note N).

275 **Methylation implicated in karyollele specific expression**

276 To investigate the biological mechanism causing differential expression, we measured
277 methylation on the A15 genome. Assuming that the relative Cytosine/Thymine coverage at each
278 base relates to a differential methylation state between the two nuclear types, we conclude that
279 277 genes are differentially methylated (Methods). 42 of these 277 genes were also found to be
280 differentially expressed between the two nuclear types at some point in development. Although
281 this is a significant proportion ($p < 0.05$, χ^2 test, Supplementary Material Note O), methylation
282 only explains at most 10% of the differential expression we observe. Noteworthy is that 40 of the
283 42 differentially expressed and differentially methylated genes are differentially expressed in
284 mushroom tissues (Supplementary Material Note O), whereas only 9 are differentially expressed
285 in the vegetative mycelium. This indicates that the largest impact of differential methylation is
286 much later in mushroom development, suggesting that methylation has a delayed effect on
287 expression.

288 **Discussion**

289 Differently from most eukaryotes, nuclei remain side by side during most of the life cycle of
290 basidiomycete fungi. Whether each nucleus is contributing equally to the phenotype and, if not,
291 how this is regulated is largely unknown. In an attempt to understand this, we studied the
292 expression of alleles in both constituent nuclei (P1 and P2) of the button mushroom cultivar
293 Sylvan 15. From the observed average gene expression, we conclude that the expression of
294 nuclear type P1 of the *Agaricus bisporus sylvan A15 strain* is dominant over nuclear type P2.
295 Remarkably, this dominance is present across all developmental stages in the heterokaryon. We
296 can link this phenomenon to the human case, where in fibroblasts²⁹, it has been shown that

297 individual cells preferentially express one allele over the other, which is not evident over a
298 collection of many cells. Whereas in a diploid genome the cell must rely on heterochromatin
299 DNA packing and RNAi regulatory pathways³⁰, heterokaryotic cells could instead control the
300 energy usage of a specific nuclear type.

301 In the mushroom tissue dataset, the number of up-regulated karyolleles in P1 is approximately
302 equal to those in P2, but in the vegetative mycelium dataset, P2 has more up-regulated
303 karyolleles relative to P1. The contrast between a dominant P1, yet more differentially over-
304 expressed genes in P2 in mushroom tissue is paradoxical. However, there are many genes that
305 show a consistently higher expression in either P1 or P2, with more genes showing a consistently
306 higher expression for P1. Is it possible that the P1 homokaryon is responsible for the basal
307 mRNA production, while P2 plays a more reactive regulatory role? Mechanisms for this kind of
308 regulation are not known. In plants, sub-genome dominance may be linked to methylation of
309 transposable elements²⁴. Might it be possible that something similar happens in *A. bisporus*?

310 Although an imbalance in the number of nuclei could very well explain the dominance of P1, we
311 have shown that genes that are consistently higher expressed in one of the karyolleles do co-
312 localize in sub-chromosomal regions. If there were more P1 nuclei than P2 nuclei, we would
313 have expected a general higher expression of genes of one nuclear type across all chromosomes,
314 which we do not observe.

315 For many differentially expressed genes, the protein sequence differences between the two
316 karyolleles in the two nuclear types encode for different protein domains. This suggests a
317 functional impact of karyollele specific expression. We also observe a broad range of
318 functionality being differentially expressed between the P1 and the P2 nuclear types. For

319 example, the P2 upregulation of cazymes and metabolic genes in P2 in compost highlight the
320 importance of the P2 homokaryon in development. H97, one of the homokaryons in the cultivar
321 Horst U1, from which Sylvan A15 is derived, displays stronger vegetative growth characteristics
322 than its counterpart H39¹. This metabolic strength may be passed down from the H97
323 homokaryon to the Sylvan A15 P2 homokaryon, and the differentially expressed karyolleles may
324 in part be responsible for this. *mnp1*, for example, is an important gene for growth on compost
325 and P2 has indeed inherited the relevant chromosome 2 from H97 (Sonnenberg et al., 2016).
326 Such characteristics are relevant for breeding strategies.

327 Surprisingly, *mnp1* is expressed and even up-regulated in the mushroom tissues. *mnp1* is known
328 to be involved in lignin degradation, which occurs in the vegetative mycelium^{2,28}. In compost,
329 the abundance decreases dramatically throughout development (Supplementary Material Note
330 K). Therefore, the abundance of *mnp1* in the stipe of the fruiting body is unexpected, although it
331 has been shown that proteins produced in the mycelium can find their way into the mushroom³¹.
332 However, it does not explain the fact that the P1 karyollele exists in higher abundance in the
333 mushroom tissues, while the P2 karyollele is higher expressed in the vegetative mycelium.
334 Transport of the P2 karyollele from the vegetative mycelium into the mushroom conflicts with
335 the abundances of the P1 karyollele observed in the mushroom tissues.

336 A significant proportion of differentially methylated karyolleles were also differentially
337 expressed, most differentially expressed genes are not observed to be methylated. The overlap
338 we observe between methylated genes and differentially expressed genes in different
339 developmental stages explain an effect in the mushroom tissue. However, we cannot link the
340 methylation to a preference of nuclear type. For example, the five differentially expressed genes
341 between compost and mushroom that change their nuclear dominance are not methylated.

342 Although, methylation seems to play a role in the differential use of nuclear type for mRNA
343 production, it only explains 10% of the observed differential expression. This may be due to a
344 limitation of our methylation dataset, (which only comprises vegetative growth), but it may also
345 hint towards other regulatory mechanisms.

346 In addition to methylation, we also observe co-localization of co-expressed genes. This may be
347 indicative of a difference in genome organization, whereby the DNA is less accessible in certain
348 regions in P1 than in P2 through different levels of chromatin compaction. It has been shown that
349 gene expression is strongly linked to DNA availability, and further, that such chromatin
350 organization is heritable³².

351 The sequences of a pair of karyolleles need to be sufficiently different for our algorithm to be
352 able to uniquely assign reads to each karyollele. These sequence differences between nuclear
353 types may have an effect on various regulatory mechanisms of transcription, such as
354 transcription factor binding efficiencies, transcription efficiency, differences in mRNA stability,
355 or differences in epigenetic factors. Future research might shed light on whether these
356 differences are related to observed differential karyollele expression.

357 Causative mechanisms of karyollele specific expression can further be elucidated by population
358 studies across multiple spore isolates. Sylvan A15 is derived as a heterokaryotic single spore
359 isolate from Horst U1. In such heterokaryons, non-sister nuclei are paired in one spore.

360 Combined with the restriction of recombination to chromosome ends, such heterokaryons are
361 genetically very similar to the parent and differ only in the distribution of parental type
362 chromosomes over both nuclei. Karyollele expression could thus be studied in different
363 heterokaryotic single spore isolates having different distributions of otherwise very similar

364 chromosomes over both nuclei. If the expression patterns are consistent with nuclear
365 chromosome organization across different single spore isolates, it will suggest that expression of
366 specific karyolleles can be controlled by selecting isolates where karyolleles lie in the desired
367 nuclei.

368 **Conclusion**

369 We show that karyolleles, the different copies of a gene separated by nuclear membranes in a
370 heterokaryon, are differentially expressed between the two different nuclear types in the
371 *Agaricus bisporus Sylvan A15 strain*. Each nuclear type contributes varying amounts of mRNA
372 to the cell, and differential expression occurs at the gene level. Despite a dominant P1 type, we
373 see no evidence that would suggest an imbalance in the number of copies P1 and P2 nuclei in
374 any cell type, though it may vary from cell to cell.

375 Genes with various vital functions are differentially expressed. The P2 homokaryon significantly
376 up-regulates cazymes and metabolic genes, which may indicate a difference in vegetative growth
377 strengths. This corroborates what was observed in the constituent homokaryons of the Horst U1
378 cultivar from which P1 and P2 are essentially derived.. Manganese peroxidase is one of the
379 differentially expressed genes, and exhibits interesting, previously unknown behavior. The cause
380 of these differential regulations is still not known, but it is possible that epigenetic mechanisms,
381 like methylation, play a role.

382 The biological gene regulation mechanisms between heterokaryons need to be investigated.
383 Unfortunately, such research is hindered by current mRNA isolation procedures. As mRNA
384 transcripts are secreted from the nuclei and mixed in the cytoplasm of the cell, traditional
385 sequencing methods will be unable to generate a full resolution of both homokaryon expression

386 from full cell isolates. Single nucleus sequencing^{33,34} would circumnavigate this issue by
387 isolating mRNA from individual nuclei. As we have shown that the two nuclear types exhibit
388 distinguishable regulatory programs, it will be possible to distinguish them based on their
389 expression profiles.

390 The impact of differential expression between nuclei of heterokaryotic organisms is
391 underappreciated. Heterokaryotic fungi have major impact in clinical and biotechnological
392 applications, and impact our economy and society as animal pathogens such as *Cryptococcus*
393 *neoformans*³⁵, plant pathogens such as *Ustilago maydis*³⁶, plant and soil symbionts such as
394 mycorrhizal fungi²⁶, bioreactors such as *Schizophyllum commune*³⁷, and of course the subject of
395 this study, the cultivated, edible mushroom *Agaricus bisporus*¹⁵. It is known that different
396 homokaryons in these species will produce different phenotypes² which no doubt need to be
397 treated, nourished or utilized differently.

398 We have demonstrated differential nuclear regulation of a fungal organism and we showed that
399 variation between homokaryons results in functional differences that were previously unknown.
400 With this work, we hope to draw attention to the impact of sequence and regulatory variation in
401 different nuclei on the function and behavior of the cell in order to further our understanding of
402 the role of fungi in our environment.

403 **Materials and Methods**

404 **RNA-Seq data:** We used two RNA-seq datasets from the *Agaricus bisporus* (A15) strain: (1)
405 tissue samples through mushroom development (BioProject: PRJNA309475)²⁷, and (2)
406 vegetative mycelium samples taken from compost through mushroom development (BioProject
407 PRJNA275107)². Throughout the text, when we refer to the mushroom tissue, we also refer to all

408 samples in dataset (1), including the first sample, which technically is a sample of the vegetative
409 mycelium. The compost dataset exhibited high amounts of PCR duplicates (Supplementary
410 Material Note P). This can be attributed to the difficulty in isolating RNA from soil. To remedy
411 the biases involved with this, we removed all PCR duplicates using FastUniq³⁸.

412 **Methylation data:** A sample of vegetative stage mycelium of A15 was treated with the EpiTect
413 Bisulphite conversion and cleanup kit and sequenced with the Illumina HiSeq 2000. Raw reads
414 were trimmed using TRIMMOMATIC³⁹ and aligned to the A15 P1 genome using Bismark⁴⁰ and
415 bowtie2⁴¹. Methylated bases were analyzed with Methylkit⁴². Only bases which had a minimum
416 coverage of 10 were retained. For samples with mixed methylation states, we will observe what
417 appear to be incomplete conversions of unmethylated cytosines but in reality represents the
418 mixed methylation states of those bases. Therefore, to include only differentially methylated
419 bases between the two nuclei (i.e. methylated in one homokaryon, but not in the other), we
420 considered only those bases which were measured to be methylated between 40 and 60% of all
421 reads (Supplementary Material Note O). While 164,290 bases had an indication of methylation
422 signal, 10,325 bases had methylation signals of about 50%, suggestive of differential methylation
423 states. Methylated bases were mapped to genes when between the start and stop codons, or
424 1000bp up/downstream (Supplementary Material Note Q).

425 **Homokaryon genome and annotations:** The P1 and P2 genomes¹⁵ were annotated with
426 BRAKER1[21] using the pooled RNA-seq data described above. In order to prevent chimeric
427 genes (neighboring genes that are erroneously fused into one predicted gene) the following
428 procedure was used. After the first round of gene prediction, predicted introns were identified
429 that were at least 150 bp in size and not supported by RNA-seq reads. The midpoint of these
430 introns were labeled as intergenic regions in the next round of gene prediction using

431 AUGUSTUS 3.0.2⁴³ and the parameter set produced in the first round of gene prediction. The
432 SNP density between the genomes was estimated using MUMMER's⁴⁴ show-snps tool.

433 **Karyollele pair discovery:** The genome annotations were used to produce predicted mRNA
434 sequences for each gene. The genes in the two parental genomes were matched using a reciprocal
435 best BLAST⁴⁵ hit. Hits which had E-values greater than 10^{-100} were removed. This resulted in a
436 conservative orthology prediction between the two homokaryons that are our set of karyolleles.
437 Karyollele pairs which have a 100% sequence identity were removed, as it would be impossible
438 to identify distinguishing markers for these identical pairs.

439 **Marker Discovery:** For each discovered karyollele pair, we identify markers that uniquely
440 identify each element of the pair. This is done by constructing all possible kmers for each
441 sequence, resulting in two sets per pair. The kmers overlapping in these sets are removed,
442 resulting in distinguishing pairs of markers. Once distinguishing markers have been discovered
443 for all pairs, we remove all non-unique markers. Finally, the set of markers is made non
444 redundant by scanning the position-sorted list of markers from left to right and removing any
445 marker that overlaps with the previous marker. Finally, we ensure that the markers are unique
446 throughout the whole genome by removing markers that are present anywhere else in either
447 genome. In order to guarantee sufficient evidence across the whole gene, we remove karyollele
448 pairs which do not have at least five markers each.

449 **Marker quantification:** We scan all RNA-Seq reads for the detected markers using the Aho-
450 Corasick algorithm⁴⁶. We insert all markers and their reverse complements into an Aho-Corasick
451 tree and count each marker only once for each fragment (a marker may be present twice, if the
452 read mates overlap). We calculate a gene expression score as the average of each marker count

453 for a gene. This results in an expression score E_h for each gene g in each sample t for each
454 replicate r , per homokaryon h :

$$455 \quad E_h(r, s, g) = \frac{1}{|M_h(g)|} \sum_{m \in M_h(g)} C_h(r, s, m) \quad (1)$$

456 where $M_h(g)$ is the set of markers in a gene g , and $C_h(r, s, m)$ is the count for marker m in replicate
457 r , sample s .

458 **Differential expression:** Using DE-Seq⁴⁷, we perform a differential expression test for each
459 karyotype pair in a tissue, i.e. we test if a gene has a differential expression in P1 or P2. DESeq
460 requires a size factor to be calculated, which normalizes for the library sizes of each sample.
461 Since however, the counts from P1 and from P2 originate from the same sample, these must have
462 the same size factor. Size factors are therefore calculated manually, by counting the total number
463 of reads for each sample, and dividing it by the largest value for any sample (Equation 2).

$$464 \quad sf(s, r) = \frac{\sum_h \sum_{m \in M_h(g)} C_h(r, s, m)}{\max_{(s', r')} \left(\sum_h \sum_{m \in M_h(g)} C_h(r', s', m) \right)} \quad (2)$$

465 The P1 and P2 counts originating from the same sample will then be assigned the same size
466 factor. The expression counts for each gene in each replicate in each tissue (equation 1) are
467 provided to DE-Seq with the provided size factor (Equation 2). The normalized read counts per
468 gene $D_h(s, g)$ are returned by DE-Seq, together with significance values for each test. We select
469 only differentially expressed genes that have a q-value < 0.05 , and a fold change of at least three.

470 **Read ratio calculation:** Using the normalized read counts from DE-Seq⁴⁷, we calculate the
471 ratio of the number of reads originating from the two homokaryons at the gene (GRR),
472 chromosome (CRR) and nuclear type level (NRR).

473

$$GRR(s, g) = \frac{D_{P1}(s, g)}{D_{P2}(s, g)} \quad (3)$$

$$CRR(s, c) = \frac{\sum_{g \in c} D_{P1}(s, g)}{\sum_{g \in c} D_{P2}(s, g)} \quad (4)$$

$$NRR(s) = \frac{\sum_{c \in C} \sum_{g \in c} D_{P1}(s, g)}{\sum_{c \in C} \sum_{g \in c} D_{P2}(s, g)} \quad (5)$$

474

475 **Gene ratio calculation:** Using the normalized read counts from DESeq⁴⁷, we calculate the ratio
476 of the number of reads originating from the two homokaryons at the gene level, and use those
477 ratios to calculate the geometric mean of the relative expression activities at the chromosome
478 (CGR, Equation 6) and nuclear type level (NGR, Equation 7). The geometric mean is more
479 suitable than the arithmetic mean for averaging ratios.

$$CGR(s, c) = \sqrt[|c|]{\prod_{g \in c} GRR(s, g)} \quad (6)$$

$$NGR(s) = \sqrt[|C|]{\prod_{c \in C} CGR(s, c)} \quad (7)$$

480

481 **Identifying consistent genes:** For each gene, we observe the relative expression in each sample
482 (Equation 3). We refer to a gene as being consistently expressed if it is more highly expressed in
483 the same nuclear type in each sample. I.e. the GRR is always greater than one, or always less
484 than 1.

485 **Identifying co-regulated clusters:** We slide a window of size 20,001bp (10,000- up and down-
486 stream) across each chromosome. In this window, we count the number of genes that are more
487 highly expressed by P1 and by P2, and calculate the difference per sample. I.e.

$$488 \quad D(x, s) = \sum_{g \in W(x-10000, x+10000)} \begin{cases} 1 & \text{if } GRR(g, s) > 1 \\ -1 & \text{if } GRR(g, s) < 1 \end{cases} \quad (8),$$

489 where $W(x,y)$ is the set of genes between genomic location x and y , and s is a sample. This
490 difference is shown in Figure 5. Next, we identify regions where each sample in the dataset
491 shows consistent regulation. That is to say, in these regions, $D(x,s) > 0 \forall s \in S$, or $D(x,s) < 0 \forall s$
492 $\in S$, where S is the set of all samples. These regions contain co-localized genes that are co-
493 regulated across all samples.

494 **Functional predictions:**

495 **PFAM:** Conserved protein domains were predicted using PFAM version 27^{48,49}.

496 **Transcription factor definitions:** Predicted proteins with a known transcription factor-related
497 (DNA-binding) domain (based on the PFAM annotations) were considered to be transcription
498 factors.

499 **Carbohydrate-active enzymes prediction:** Using the Cazymes Analysis Toolkit (CAT)⁵⁰, we
500 predicted carbohydrate-active enzymes based on the original gene definitions. If a gene's protein
501 sequence was predicted to be a cazyme by either the sequence-based annotation method or the
502 PFAM-based annotation method then we considered it a cazyme.

503 **Secreted Proteins prediction:** We used the same procedure as ⁵¹ to predict secreted proteins.
504 Briefly, genes with SignalP ⁵² signal peptides, or a TargetP ⁵³ Loc=S were kept. The remaining
505 genes were further filtered with TMHMM ⁵⁴, keeping only genes with zero or one
506 transmembrane domains. Finally, genes were filtered using Wolf PSort ⁵⁵ to select genes with a
507 Wolf PSort extracellular score greater than 17.

508 **Metabolic and Cytochrome P450 gene groups:** Genes with the GO annotation “metabolic
509 process” (annotation ID: GO:0008152) were called as metabolism genes. Genes with the PFAM
510 annotation PF00067 were used as Cytochrome P450 genes.

511 **KEGG:** KEGG annotations were made with the KAAS KEGG ⁵⁶ annotation pipeline, using
512 genes from all available fungi, with the exception of leotiomycetes, Dothideomycetes, and
513 Microsporidians, due to the limitation of the number of species (Selected organisms by ID: cne,
514 cgi, ppl, mpr, scm, uma, mgl, sce, ago, kla, vpo, zro, cgr, ncs, tpf, ppa, dha, pic, pgu, lel, cal, yli,
515 clu, ncr, mgr, fgr, nhe, maw, ani, afm, aor, ang, nfi, pcs, cim, cpw, pbl, ure, spo, tml). The
516 GHOSTX and BBH options were selected. Predictions were made individually for both the P1
517 and P2 genomes, using the translated protein sequences.

518 **Named genes:** Named genes for *Agaricus bisporus* version 2 were downloaded from the JGI
519 DOE Genome Portal ([http://genome.jgi.doe.gov/pages/search-for-](http://genome.jgi.doe.gov/pages/search-for-genes.jsf?organism=Agabi_varbisH97_2)
520 [genes.jsf?organism=Agabi_varbisH97_2](http://genome.jgi.doe.gov/pages/search-for-genes.jsf?organism=Agabi_varbisH97_2)) by searching for genes with ‘Name’ in the ‘user
521 annotations’ attribute. Gene names were transferred from *A. bisporus* v. 2 using reciprocal best
522 blast hit to P1 and P2, and then selecting the best match (in the single case of an ambiguity). See
523 Supplementary Material Note R.

524 **Software and code availability:** Marker discovery and abundance calculations was done in
525 Scala, while downstream analysis was performed in python using the ibidas data query and
526 manipulation suite⁵⁷. All source code, together with a small artificial example dataset is
527 available at: <https://github.com/thiesgehrmann/Homokaryon-Expression>

528 **Data Availability:** The RNA-Seq data was previously generated and can be found at bioprojects
529 PRJNA309475 and PRJNA275107. The bisulphite sequencing data can be accessed at
530 SAMN06284058.

531 **Supplementary information:** Together with this manuscript, we provide a file of
532 Supplementary Notes, and Supplementary Tables 1-4 to support our findings.

533 **Acknowledgements**

534 The authors would like to thank Brian Lavrijssen for providing the bisulphite sequencing data to
535 determine the differential methylation states. The sequence and annotation data of *A. bisporus*
536 H97 version 2 were produced by the US Department of Energy Joint Genome Institute
537 <http://www.jgi.doe.gov/> in collaboration with the user community. This research is supported by
538 the Dutch Technology Foundation STW, which is part of the Netherlands Organisation for
539 Scientific Research (NWO), and which is partly funded by the Ministry of Economic Affairs.

540 **Author contributions**

541 TG, HABW, MJTR and TA wrote the manuscript. JFP performed the experiments. TG, HABW,
542 MJTR and TA designed the analyses. RAO created the gene and functional annotations. TG
543 performed the analyses. All authors aided in biological interpretation of the results. All authors
544 reviewed the manuscript.

545 **References**

- 546 1. Morin, E. *et al.* Genome sequence of the button mushroom *Agaricus bisporus* reveals
547 mechanisms governing adaptation to a humic-rich ecological niche. *Proc. Natl. Acad. Sci.*
548 **109**, 17501–17506 (2012).
- 549 2. Patyshakuliyeva, A. *et al.* Uncovering the abilities of *Agaricus bisporus* to degrade plant
550 biomass throughout its life cycle. *Environ. Microbiol.* **17**, 3098–3109 (2015).
- 551 3. Ohm, R. a *et al.* Genome sequence of the model mushroom *Schizophyllum commune*.
552 *Nat. Biotechnol.* **28**, 957–63 (2010).
- 553 4. Pawlowska, T. E. Genetic processes in arbuscular mycorrhizal fungi. *FEMS Microbiol.*
554 *Lett.* **251**, 185–192 (2005).
- 555 5. ud din Khanday, M. *et al.* in *Soil Science: Agricultural and Environmental Prospectives*
556 317–332 (Springer International Publishing, 2016). doi:10.1007/978-3-319-34451-5_14
- 557 6. Sun, C. *et al.* The beneficial fungus *Piriformospora indica* protects *Arabidopsis* from
558 *Verticillium dahliae* infection by downregulation plant defense responses. *BMC Plant*
559 *Biol.* **14**, 268 (2014).
- 560 7. Harrach, B. D., Baltruschat, H., Barna, B., Fodor, J. & Kogel, K.-H. The mutualistic
561 fungus *Piriformospora indica* protects barley roots from a loss of antioxidant capacity
562 caused by the necrotrophic pathogen *Fusarium culmorum*. *Mol. Plant. Microbe. Interact.*
563 **26**, 599–605 (2013).
- 564 8. Babikova, Z. *et al.* Underground signals carried through common mycelial networks warn

- 565 neighbouring plants of aphid attack. *Ecol. Lett.* n/a-n/a (2013). doi:10.1111/ele.12115
- 566 9. Collins, C. *et al.* Genomic and proteomic dissection of the ubiquitous plant pathogen,
567 armillaria mellea: Toward a new infection model system. *J. Proteome Res.* **12**, 2552–2570
568 (2013).
- 569 10. Khoshraftar, S. *et al.* Sequencing and annotation of the *Ophiostoma ulmi* genome. *BMC*
570 *Genomics* **14**, 162 (2013).
- 571 11. Guo, L. *et al.* Genome and transcriptome analysis of the fungal pathogen fusarium
572 oxysporum f. Sp. Cubense causing banana vascular wilt disease. *PLoS One* **9**, (2014).
- 573 12. Specht, C. A. Isolation of the Ba and Bb mating-type loci of *Schizophyllum commune*.
574 *Curr. Genet.* **28**, 374–379 (1995).
- 575 13. Saksena, K. N., Marino, R., Haller, M. N. & Lemke, P. a. Study on development of
576 *Agaricus bisporus* by fluorescent microscopy and scanning electron microscopy. *J.*
577 *Bacteriol.* **126**, 417–428 (1976).
- 578 14. Craig, G. D., Newsam, R. J., Gull, K. & Wood, D. A. An ultrastructural and
579 autoradiographic study of stipe elongation in *Agaricus bisporus*. *Protoplasma* **98**, 15–29
580 (1979).
- 581 15. Sonnenberg, A. S. M. *et al.* A detailed analysis of the recombination landscape of the
582 button mushroom *Agaricus bisporus* var. *bisporus*. *Fungal Genet. Biol.* **93**, 35–45 (2016).
- 583 16. Todd, R. B., Davis, M. a & Hynes, M. J. Genetic manipulation of *Aspergillus nidulans*:
584 heterokaryons and diploids for dominance, complementation and haploidization analyses.
585 *Nat. Protoc.* **2**, 822–830 (2007).

- 586 17. Boon, E., Zimmerman, E., Lang, B. F. & Hijri, M. Intra-isolate genome variation in
587 arbuscular mycorrhizal fungi persists in the transcriptome. *J. Evol. Biol.* **23**, 1519–1527
588 (2010).
- 589 18. James, T. Y., Stenlid, J., Olson, J. K. & Johannesson, H. Evolutionary significance of
590 imbalanced nuclear ratios within heterokaryons of the basidiomycete fungus
591 *Heterobasidion parviporum*. *Evolution (N. Y.)*. **62**, 2279–2296 (2008).
- 592 19. Muzzey, D., Sherlock, G. & Weissman, J. S. Extensive and coordinated control of allele-
593 specific expression by both transcription and translation in *Candida albicans*. *Genome Res.*
594 **24**, 963–973 (2014).
- 595 20. Wei, X. & Wang, X. A computational workflow to identify allele-specific expression and
596 epigenetic modification in maize. *Genomics. Proteomics Bioinformatics* **11**, 247–52
597 (2013).
- 598 21. Crowley, J. J. *et al.* Analyses of allele-specific gene expression in highly divergent mouse
599 crosses identifies pervasive allelic imbalance. *Nat. Genet.* **47**, 353–360 (2015).
- 600 22. Buckland, P. R. Allele-specific gene expression differences in humans. *Hum. Mol. Genet.*
601 **13**, 255–260 (2004).
- 602 23. Pant, P. V. K. *et al.* Analysis of allelic differential expression in human white blood cells.
603 *Genome Res.* **16**, 331–339 (2006).
- 604 24. Edger, P. P., Smith, R., Mckain, M. R., Cooley, A. M. & Vallejo-marin, M. Subgenome
605 dominance in an interspecific hybrid , synthetic allopolyploid , and a 140 year old
606 naturally established neo-allopolyploid monkeyflower. *bioRxiv* 1–27 (2016).

607 doi:10.1101/094797

- 608 25. Horton, T. R. The number of nuclei in basidiospores of 63 species of ectomycorrhizal
609 Homobasidiomycetes. *Mycologia* **98**, 233–238 (2006).
- 610 26. Lin, K. *et al.* Single Nucleus Genome Sequencing Reveals High Similarity among Nuclei
611 of an Endomycorrhizal Fungus. *PLoS Genet.* **10**, (2014).
- 612 27. Pelkmans, J. F. *et al.* The transcriptional regulator c2h2 accelerates mushroom formation
613 in *Agaricus bisporus*. *Appl. Microbiol. Biotechnol.* **2**, (2016).
- 614 28. Bonnen, A. M., Anton, L. H., Orth, A. B., Anton, L. L. H. & Orth, A. N. N. B. Lignin-
615 Degrading Enzymes of the Commercial Lignin-Degrading Enzymes of the Commercial
616 Button Mushroom, *Agaricus bisporus*. *Appl. Environ. Microbiol.* **60**, (1994).
- 617 29. Borel, C. *et al.* Biased allelic expression in human primary fibroblast single cells. *Am. J.*
618 *Hum. Genet.* **96**, 70–80 (2015).
- 619 30. Volpe, T. A. *et al.* Regulation of heterochromatic silencing and histone H3 lysine-9
620 methylation by RNAi. *Science* **297**, 1833–7 (2002).
- 621 31. Woolston, B. M. *et al.* Long-distance translocation of protein during morphogenesis of the
622 fruiting body in the filamentous fungus, *agaricus bisporus*. *PLoS One* **6**, (2011).
- 623 32. McDaniel, R. *et al.* Heritable Individual-Specific and Allele-Specific Chromatin
624 Signatures in Humans. *Science (80-.)*. **328**, 235–239 (2010).
- 625 33. Lake, B. B. *et al.* Neuronal subtypes and diversity revealed by single-nucleus RNA
626 sequencing of the human brain. *Science (80-.)*. **352**, 1586–1590 (2016).

- 627 34. Krishnaswami, S. R. *et al.* Using single nuclei for RNA-seq to capture the transcriptome
628 of postmortem neurons. *Nat. Protoc.* **11**, 499–524 (2016).
- 629 35. Loftus, B. J. *et al.* The genome of the basidiomycetous yeast and human pathogen
630 *Cryptococcus neoformans* TL - 307. *Science (80-.)*. **307** VN-, 1321–1324 (2005).
- 631 36. Kämper, J. *et al.* Insights from the genome of the biotrophic fungal plant pathogen
632 *Ustilago maydis*. *Nature* **444**, 97–101 (2006).
- 633 37. Shu, C. H. & Hsu, H. J. Production of schizophyllan glucan by *Schizophyllum commune*
634 ATCC 38548 from detoxified hydrolysate of rice hull. *J. Taiwan Inst. Chem. Eng.* **42**,
635 387–393 (2011).
- 636 38. Xu, H. *et al.* FastUniq: A Fast De Novo Duplicates Removal Tool for Paired Short Reads.
637 *PLoS One* **7**, 1–6 (2012).
- 638 39. Bolger, A. M., Lohse, M. & Usadel, B. Trimmomatic: A flexible trimmer for Illumina
639 sequence data. *Bioinformatics* **30**, 2114–2120 (2014).
- 640 40. Krueger, F. & Andrews, S. R. Bismark: A flexible aligner and methylation caller for
641 Bisulfite-Seq applications. *Bioinformatics* **27**, 1571–1572 (2011).
- 642 41. Langmead, B. & Salzberg, S. L. Fast gapped-read alignment with Bowtie 2. *Nat. Methods*
643 **9**, 357–359 (2012).
- 644 42. Akalin, A. *et al.* methylKit: a comprehensive R package for the analysis of genome-wide
645 DNA methylation profiles. *Genome Biol.* **13**, R87 (2012).
- 646 43. Stanke, M., Diekhans, M., Baertsch, R. & Haussler, D. Using native and syntenically

- 647 mapped cDNA alignments to improve de novo gene finding. *Bioinformatics* **24**, 637–644
648 (2008).
- 649 44. Kurtz, S. *et al.* Versatile and open software for comparing large genomes. *Genome Biol.* **5**,
650 R12 (2004).
- 651 45. Altschul, S. F., Gish, W., Miller, W., Myers, E. W. & Lipman, D. J. Basic local alignment
652 search tool. *J. Mol. Biol.* **215**, 403–10 (1990).
- 653 46. Aho, A. V. & Corasick, M. J. Efficient string matching: an aid to bibliographic search.
654 *Commun. ACM* **18**, 333–340 (1975).
- 655 47. Anders, S. *et al.* Differential expression analysis for sequence count data. *Genome Biol.*
656 **11**, R106 (2010).
- 657 48. Finn, R. D. *et al.* The Pfam protein families database. *Nucleic Acids Res.* **36**, D281–D288
658 (2008).
- 659 49. Finn, R. D. *et al.* Pfam: The protein families database. *Nucleic Acids Res.* **42**, 222–230
660 (2014).
- 661 50. Lombard, V., Golaconda Ramulu, H., Drula, E., Coutinho, P. M. & Henrissat, B. The
662 carbohydrate-active enzymes database (CAZy) in 2013. *Nucleic Acids Res.* **42**, D490–
663 D495 (2014).
- 664 51. Morais do Amaral, A., Antoniw, J., Rudd, J. J. & Hammond-Kosack, K. E. Defining the
665 Predicted Protein Secretome of the Fungal Wheat Leaf Pathogen *Mycosphaerella*
666 *graminicola*. *PLoS One* **7**, 1–19 (2012).

- 667 52. Petersen, T. N., Brunak, S., von Heijne, G. & Nielsen, H. SignalP 4.0: discriminating
668 signal peptides from transmembrane regions. *Nat. Methods* **8**, 785–786 (2011).
- 669 53. Emanuelsson, O., Nielsen, H., Brunak, S. & von Heijne, G. Predicting Subcellular
670 Localization of Proteins Based on their N-terminal Amino Acid Sequence. *J. Mol. Biol.*
671 **300**, 1005–1016 (2000).
- 672 54. Krogh, A., Larsson, B., von Heijne, G. & Sonnhammer, E. L. . Predicting transmembrane
673 protein topology with a hidden markov model: application to complete genomes. *J. Mol.*
674 *Biol.* **305**, 567–580 (2001).
- 675 55. Horton, P. *et al.* WoLF PSORT: protein localization predictor. *Nucleic Acids Res.* **35**,
676 W585–W587 (2007).
- 677 56. Moriya, Y., Itoh, M., Okuda, S., Yoshizawa, A. C. & Kanehisa, M. KAAS: An automatic
678 genome annotation and pathway reconstruction server. *Nucleic Acids Res.* **35**, 182–185
679 (2007).
- 680 57. Hulsman, M., Bot, J. J., Vries, A. P. de & Reinders, M. J. T. Ibibas: Querying Flexible
681 Data Structures to Explore Heterogeneous Bioinformatics Data. *Data Integr. Life Sci.* 23–
682 37 (2013). doi:10.1007/978-3-642-39437-9_2

683

1 **Figures for “Nucleus specific expression in the multinucleated**
2 **mushroom *Agaricus bisporus* reveals different nuclear regulatory**
3 **programs”**
4

5 Thies Gehrman^{1,*}, Jordi F. Pelkmans², Robin A. Ohm², Aurin M. Vos^{2,#}, Anton S.M. Sonnenberg³,
6 Johan J.P. Baars³, Han A. B. Wösten², Marcel J. T. Reinders¹, Thomas Abeel^{1,4}

7 ¹Delft Bioinformatics Lab, Delft University of Technology, The Netherlands

8 ²Fungal Microbiology, Utrecht University, The Netherlands

9 ³Plant Breeding, Wageningen University, The Netherlands

10 ⁴Broad Institute of MIT and Harvard, USA

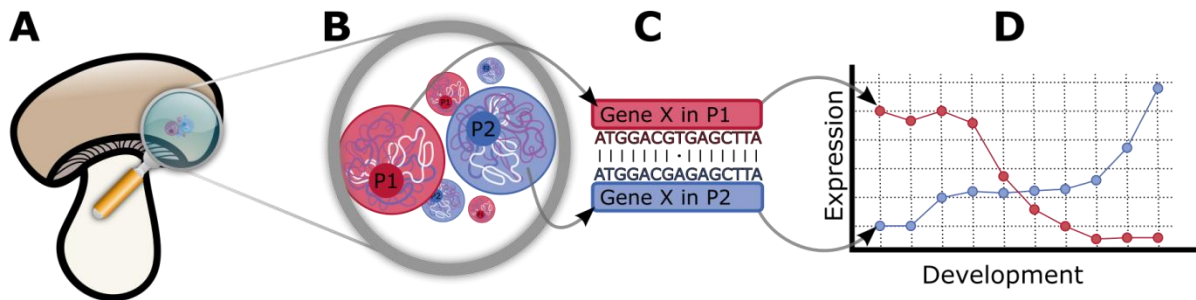
11 * Current position: CBS/KNAW Westerdijk Fungal Biodiversity Institute, The Netherlands

12 #Current position: Department of Biotechnology, Delft University of Technology, The Netherlands

13 E-mail: t.gehrmann@cbs.knaw.nl

14

15 **Figure 1**

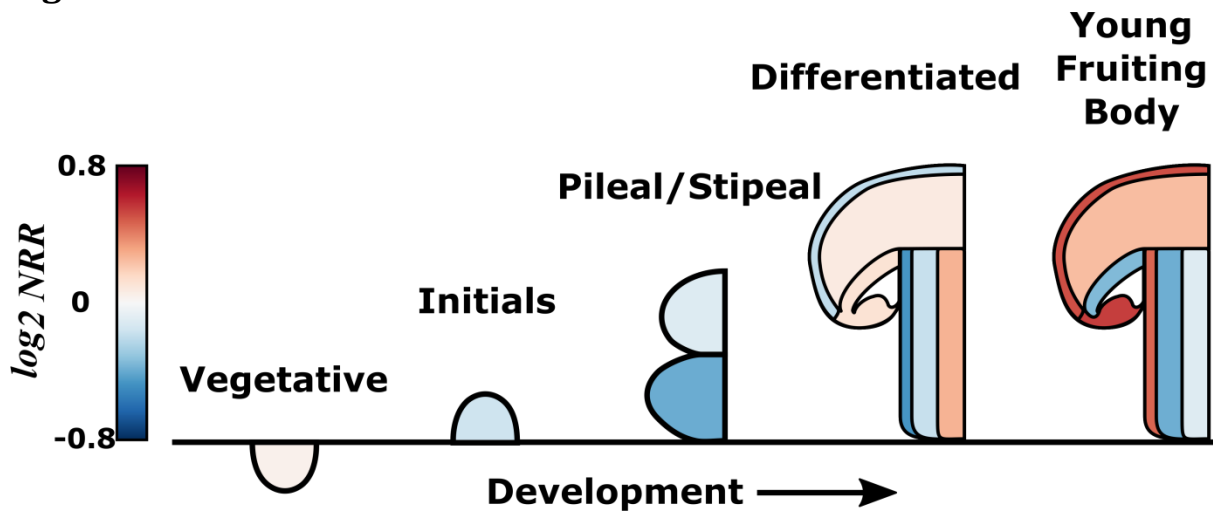


16

17 Figure 1: Nuclear type specific expression in *A. bisporus*. **A)** The *A. bisporus* mushroom is composed
18 of different tissues that consist of hyphae comprised of cellular compartments. **B)** Each cellular
19 compartment is a heterokaryon containing between 2 and 25 nuclei. In our strain, each nucleus is
20 either of type P1 (red) or P2 (blue). Both nuclear types are haploid, and contain exactly one copy of
21 each gene. However, because there are multiple nuclei, there may be multiple copies of each gene
22 in the cell. **C)** Furthermore, the gene in the two types, which we call karyolleles, may differ in their
23 genetic sequences. **D)** These differences in transcript sequence allow us to quantify expression of
24 each karyollele in each tissue and to investigate nucleus specific expression.

25

26 **Figure 2**

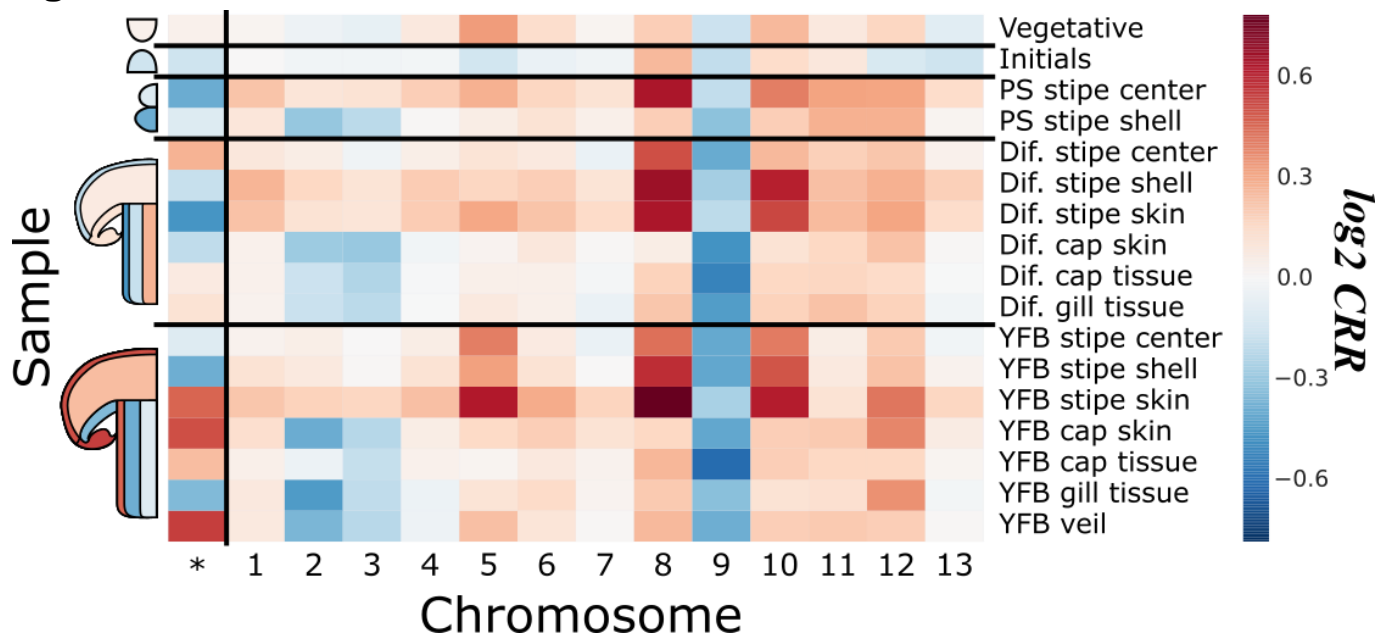


27

28 Figure 2: Read count ratios at the nuclear type level (Equation 5) of *Agaricus bisporus* throughout its
29 development. Red colour indicates higher P1 activity, blue colour higher P2 activity. The scale bar
30 indicates the \log_2 fold change in activity between the P1 and P2 nuclear types. We observe a
31 differential mRNA activity in different mushroom tissues.

32

33 **Figure 3**

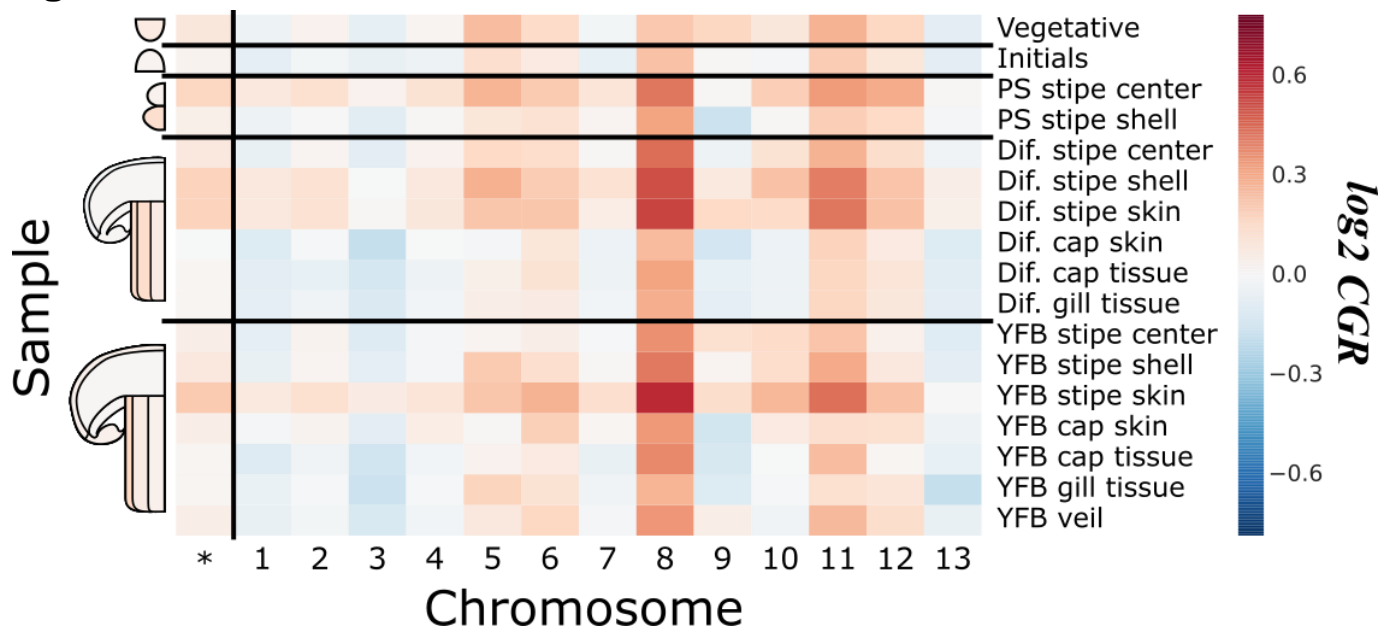


34

35 Figure 3: The read count ratios at the chromosome level (Equation 4) throughout development of
36 the mushroom. The different tissues are shown along the y-axis, and the different scaffolds are given
37 along the x-axis. Red colour indicates higher P1 activity, blue colour higher P2 activity. The first
38 column provides the read count ratios at the nuclear type level (NRR) from Figure 1. Supplementary
39 Material Note G provides the read count ratios at the chromosome level in the vegetative mycelium
40 dataset.

41

42 **Figure 4**

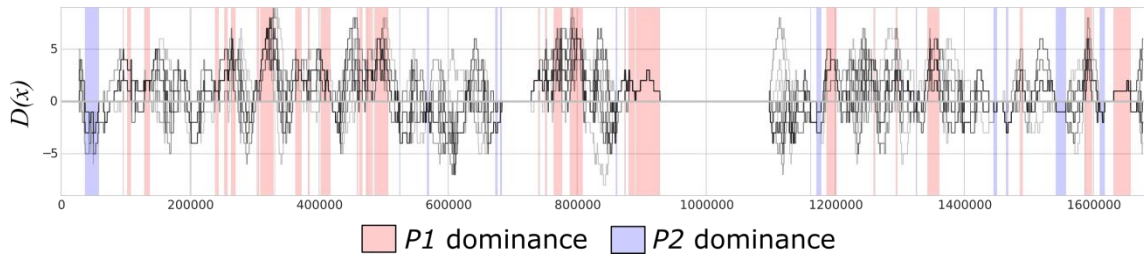


43

44 Figure 4: The chromosome gene ratios (Equation 6) per nuclear type at the chromosome level
 45 (Equation 4) (rows) and per chromosome (columns). Red colour indicates higher P1 activity, blue
 46 colour higher P2 activity. The first column (indicated with a star) represents gene ratio
 47 measurements for each tissue (see Supplementary Material Note G). P1 produces more mRNA per
 48 gene on average than P2. This is particularly striking in scaffold 8. See Supplementary Material Note
 49 H for the gene ratio measures in the vegetative mycelium dataset.

50

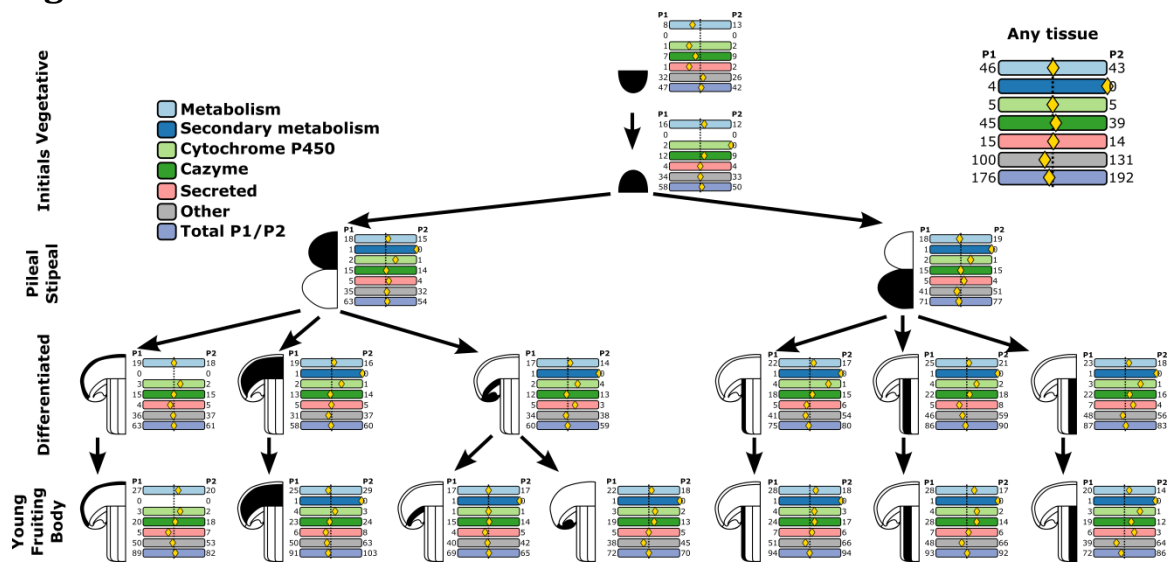
51 **Figure 5**



53 Figure 5: Co-localized genes are often co-regulated. Pictured here are the co-localized and co-
54 regulated gene clusters along chromosome 10 in the mushroom tissue dataset. Along the x-axis is
55 the genomic co-ordinate. For each sample (gray lines), we plot the difference between the number
56 of genes more highly expressed by P1 and the number of genes more highly expressed by P2 (a value
57 of 0 indicates an equal distribution). We also highlight the regions that are consistently upregulated
58 in P1 (red regions) and the number of genes that are consistently upregulated in P2 (blue regions).
59 See Supplementary Material Note J for other chromosomes.

60

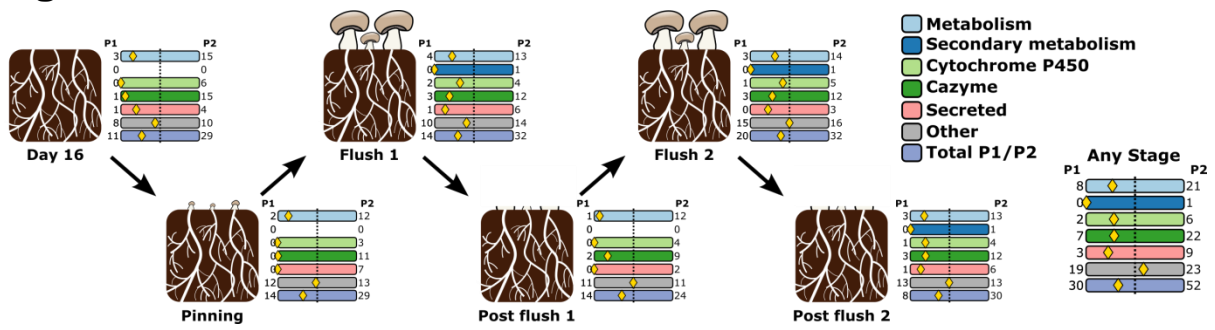
61 **Figure 6**



62

63 Figure 6: Differential regulation of functional groups through mushroom development. The
 64 development of different tissues is illustrated as a tree. We investigate metabolic genes (light blue),
 65 secondary metabolic genes (dark blue), cytochrome P450 genes (light green), carbohydrate active
 66 enzymes (dark green), secreted protein genes (light red), and all others not fitting into any of the
 67 previous groups (grey). At each developmental stage, we observe how many genes of each group are
 68 differentially upregulated in P1 (left) and in P2 (right). The yellow diamond indicates the ratio of
 69 these counts. We see that the groups are more or less equally distributed between P1 and P2 (the
 70 yellow diamond is centered), with the exception of the vegetative stage (the root node).

71 **Figure 7**



72

73 Figure 7: Differential regulation of functional groups in compost mycelium. As in figure 5, we
 74 investigated various functional groups, only here in compost. Here, however, we observe a distinct
 75 imbalance that was not present in the mushroom. The yellow diamonds are frequently left of the
 76 centre, indicating a substantial difference in the frequency of differential expression between the
 77 two nuclear types.